LAWRENCE
LIVERMORE
NATIONAL
LABORATORY

UCRL-PROC-209553

Correlation Between Two Types of Surface Stress Mitigation and the Resistance to Corrosion of Alloy 22

Ahmet Yilmaz, David V. Fix, John C. Estill, Raúl B. Rebak

February 10, 2005

ASME Presssure Vessels & Piping Division Conference
Denver, CO, United States
July 17, 2005 through July 21, 2005

CORRELATION BETWEEN TWO TYPES OF SURFACE STRESS MITIGATION AND THE RESISTANCE TO CORROSION OF ALLOY 22

Ahmet Yilmaz

David V. Fix

John C. Estill

Raúl B. Rebak

Lawrence Livermore National Laboratory
7000 East Ave, L-631
Livermore, California, 94550 USA

ABSTRACT

When metallic plates are welded, residual tensile stresses may develop in the vicinity of the weld seam. Processes such as Low Plasticity Burnishing (LPB) and Laser Shock Peening (LSP) could be applied locally to eliminate the residual stresses produced by welding. In this study, Alloy 22 (N06022) plates were welded and then the above-mentioned surface treatments were applied to eliminate the residual tensile stresses. The aim of the current study was to compare the corrosion behavior of as-welded (ASW) plates with the corrosion behavior of plates with stress mitigated surfaces. Immersion and electrochemical tests were performed. Results show that the corrosion resistance of the mitigated plates was not affected by the surface treatments applied.

Keywords: Stress Mitigation, Corrosion Rate, N06022

INTRODUCTION

Alloy 22 (N06022) has nominally 56% Nickel (Ni), 22% Chromium, 13% Molybdenum (Mo) and 3% Tungsten (W). [1] Alloy 22 is highly resistant to all types of corrosion, including environmentally assisted cracking, localized corrosion such as crevice corrosion and general or uniform corrosion. [2-4] Alloy 22 was selected for the fabrication of the outer shell of the high level nuclear waste containers for the proposed Yucca Mountain repository. [5-6] The containers will be fabricated and solution heat-treated before the waste is loaded into the containers. [6] After loading, the closure lid of the Alloy 22 containers will be welded using the gas tungsten arc welding (GTAW) process. [7] There are currently two methods under consideration to minimize or eliminate residual tensile stresses that may result from the final closure welding. These are: (1) Low Plasticity Burnishing (LPB) and (2) Laser shock Peening (LSP). These stress mitigation treatments are aimed to reducing residual surface tensile stresses that could promote the initiation of environmentally assisted cracking (EAC) in Alloy 22. [6]

It is important to know if the proposed surface treatments will affect the general and localized corrosion resistance of welded plates. The aim of this work was to evaluate comparatively the general and localized corrosion resistance of Alloy 22 in as-welded (ASW) plates and in welded plates that were treated for surface stress mitigation. Immersion and electrochemical tests were performed to assess changes in the corrosion resistance of the three studied materials.

EXPERIMENTAL

Preparation of the Welded Plates

Coupons and specimens were prepared from three differently treated welded plates of Alloy 22. Both immersion and electrochemical tests were conducted following ASTM standards. 8

As-Welded (ASW) Plates: Two 1-inch thick Alloy 22 plates (Heat XX2246BG) were GTAW welded lengthwise using 0.045-inch thick Alloy 22 wire (XX2048BG) for filler metal. Before the weld joining, each plate was approximately 16-inch long and 6-inch wide. The ASW plate used for corrosion testing was called F6 and the coupons and specimens prepared from this plate were all named starting with the letter W.

Low Plasticity Burnishing (LPB): LPB is a process by which a smooth hard ball is rolled over the surface of the metal to be burnished imparting compressive deformation. [9-10] The treatment in the studied Alloy 22 welded plates was performed in two steps using balls of two different sizes, the larger one with an effective surface area of 0.0154 inch² and the smaller one with an effective surface area of 0.00067 inch². In the first step the larger ball was rolled at a pressure of 780 ksi to create compressive stresses to a larger depth. In the second step, the smaller ball was rolled at a pressure of 821 ksi to increase the level of compressive stresses near the surface. The LPB treatment of the Alloy 22 studied plates was carried out at the Surface Enhancement Technologies Company in Cincinnati, Ohio. The burnished plate was called F4 and the coupons and specimens prepared from this plate were all named starting with the letter B.

Laser Shock Peening (LSP): Laser shock peening is a process by which a laser beam is pulsed upon a metallic surface producing a planar shockwave that travels though the work piece and plastically deforms into compressive stresses a layer of material. [11-12] The laser beam is generally applied to the work piece though a transparent overlay and an absorbent coating. A plasma forms under the overlay increasing the pressure and therefore the compressive stresses on the treated part. It has been shown specifically that a LSP treatment of 33-mm thick Alloy 22 welds actually produced a 4-mm deep layer of compressive stresses on the surface. [12] The current LSP treatment in the Alloy 22 welded plates was performed by applying laser pulses of 14 Joules for 25 nano seconds. Each spot dimension was approximately 2.5 mm square. The laser-peened plate was called F2 and the coupons and specimens prepared from this plate were all named starting with the letter P.

Immersion Corrosion Coupons

Table 1 shows the heats and the chemical composition of the plates. The plates met the specifications of ASTM B 575. [1] The plates were cut in approximately 0.5-inch thick slices perpendicular to the weld seam. There were two LPB plate slices (B9 and B10), three LSP plate slices (P13, P14 and P15) and three ASW plate slices (W13, W14 and W15). The immersion corrosion testing coupons were prepared from the above listed plate slices. The testing coupons were approximately 0.5 to 1-inch wide, 0.25 to 0.5-inch thick and 2-inch long. The 2-inch length contained the weld seam at the center and base metal at both sides of the weld seam. These sizes were constrained by the testing apparatus (ASTM G 28). 8 The surface area of the coupons varied generally from 20 to 40 cm² and the weight varied from 40 to 90 g. The coupons were degreased in acetone, rinsed in de-ionized water and let dry. Each coupon was dimensioned and weighed three times before the corrosion testing started.

Table 1.
Approximate Welded Plate Composition

Element	Plate or Base Metal Heat XX2246BG	Weld Wire or Filler Metal Heat XX2048BG
Ni	~60	59.4
Cr	20.4	20.48
Mo	13.9	14.21
W	3.3	3.02
Fe	2.3	2.53
Co	0.2	0.02
Mn	0.2	0.2
V	0.01	0.02
Cu	---	0.04

ASTM G 28 A or Ferric Sulfate + Sulfuric Acid Test: This method measures the susceptibility of nickel alloys to intergranular attack. It is often used to determine preferential intergranular attack near welds or in heat affected zones (HAZ). The guidelines are specified in the Annual Book of ASTM standards. 8 The ASTM G 28 A method for Alloy 22 consists in immersing coupons of the alloy for 24 h in a boiling solution of 42 g/L $Fe_2(SO_4)_3$ (ferric sulfate) plus 50% H_2SO_4 (sulfuric acid). The difference in the mass of the coupon between before and after the test can be used to calculate the uniform corrosion rate. Corrosion rates were calculated according to Equation 1 8

$$CR(mm/y) = \frac{8.76 \times 10^{-4} (W_i - W_f)(g)}{A(cm^2) \cdot t(h) \cdot d(g \cdot cm^{-3})} \qquad (1)$$

Where Wi is the initial weight (mass) of the coupon and Wf is the final mass, A is the surface area of the coupon, t is the testing time (24 h) and d is the density of Alloy 22 (8.69 g/cm³). [8]

The testing coupons were parallelepipeds, that is, they had six faces. Only one face is of interest (the treated one, which was either ASW, LPB or LSP). The other faces are as-cut faces and remained in the same condition for all three types of coupons. Whenever comparing surface characteristics after corrosion only the face of interest is discussed. Figure 2 shows the general appearance of three coupons after immersion testing. These coupons represent each one of the testing materials.

Electrochemical Test Specimens

Alloy 22 specimens were mainly prepared from 1-inch thick plate. Table 1 gives the heats and the chemical composition of the material for the tested specimens. The specimens were prism crevice assemblies (PCA) (Figure 3) as reported elsewhere. [13] For the current tests, the surface area of the PCA specimens was 3.27 cm². The original surface of a PCA specimen is usually 14.06 cm². [13] However for the current specimens, all the non-important surfaces were lacquered to avoid their interaction with the environment. Thus, only the ASW, LPB and LSP surfaces were exposed to the electrolyte solution for the tests. The crevicing mechanism for these PCA tests was based on ASTM G 48 12-tooth washer; however the washer was not the standard ceramic plus PTFE tape used in other tests at LLNL. [13] Since the current specimens did not have a completely smooth flat surface the crevicing washer was constructed using a hard organic material (PVDF or Polyvinylidene fluoride), which could sufficiently deform and provide a tight crevicing mechanism on an uneven surface. The PVDF washers were also coated with PTFE tape in a similar way as the ceramic washers. The PCA specimens were degreased in acetone and DI water, let dry and then all the non-important surfaces were lacquered. The lacquer was allowed to dry for at least 6 hours and then the specimens were inspected for discontinuities. The resistance of the lacquered surfaces was measured to verify electrical insulation from the electrolyte. The specimens were also inspected after the tests confirming that the lacquer did not break or disbond during testing. Specimens were used in the as-welded (ASW), in the low plasticity burnishing (LPB) and in the laser shock peened (LSP) conditions. The specimens were labeled respectively W, B and P. The weld seam run across center of the surface of the specimen that was purposely creviced with the multiple teeth washer.

Electrolyte Solutions for Electrochemical Testing

Electrochemical tests were performed in deaerated 1 M NaCl pH 6 at 90°C. Nitrogen (N2) was purged through the solution at a flow rate of 100 cc/min for 24 hours while the corrosion potential (E_{corr}) was monitored. Nitrogen bubbling was carried throughout all the electrochemical tests. The electrochemical tests were conducted in a one-liter, three-electrode, borosilicate glass flask (ASTM G 5). [8] A water-cooled condenser combined with a water trap was used to avoid evaporation of the solution and the ingress of air. The temperature of the solution was controlled by immersing the cell in a thermostatisized silicone oil bath. All the tests were carried at ambient pressure. The reference electrode was saturated silver chloride (SSC) electrode, which has a potential of 199 mV more positive than the standard hydrogen electrode (SHE). The reference electrode was connected to the solution through a water-jacketed Luggin probe so that the electrode was maintained at near ambient temperature. The counter electrode was a flag (36 cm^2) of platinum foil spot-welded to a platinum wire. All the potentials in this paper are reported in the SSC scale.

Basically, the test sequence for each specimen consisted of three parts: (1) E_{corr} evolution as a function of time for 24 h, (2) Polarization Resistance (ASTM G 59) three subsequent times and (3) A larger anodic polarization to determine susceptibility to crevice corrosion This is the Cyclic Potentiodynamic Polarization (CPP) method (ASTM G 61).

Polarization Resistance (ASTM G 59): Corrosion rates (CR) were obtained using the polarization resistance method (ASTM G 59). [8] Each one of these tests lasts approximately four minutes. An initial potential of 20 mV below the corrosion potential (E_{corr}) was ramped to a final potential of 20 mV above E_{corr} at a rate of 0.167 mV/s. Linear fits were constrained to the potential range of 10 mV below E_{corr} to 10 mV above E_{corr}. During the fitting of the data to calculate the polarization resistance (R_p), the potential (E) was plotted in the X-axis. The Tafel constants, ba and bc, were assumed to be + 0.12 V/decade. Corrosion rates were calculated using Equation 2

$$i_{corr} = \frac{1}{R_p} \times \frac{b_a \cdot b_c}{2.303(b_a + b_c)}$$

$$CR(\mu m / yr) = k \frac{i_{corr}}{\rho} EW \qquad (2)$$

Where k is a conversion factor (3.27 x 10^9 $nm \cdot g \cdot A^{-1} \cdot cm^{-1} \cdot yr^{-1}$), i_{corr} is the corrosion current density in A/cm^2 (calculated from the measurements of the resistance to polarization, R_p), EW is the equivalent weight, and is the density of Alloy 22 (8.69 g/cm^3). Assuming an equivalent dissolution of the major alloying elements as Ni^{2+}, Cr^{3+}, Mo^{6+}, Fe^{2+}, and W^{6+}, the EW for Alloy 22 is 23.28 (ASTM G 102). [8]

Cyclic Potentiodynamic Polarization - CPP (ASTM G 61): The test to assess the susceptibility of Alloy 22 to localized corrosion and passive stability was the cyclic potentiodynamic polarization technique, CPP (ASTM G 61). 8 The potential scan was started 100 mV below E_{corr} at a set scan rate of 0.167 mV/s. The scan direction was reversed when the current density reached 5 mA/cm^2 in the forward scan. Depending on

the range of applied potentials, each CPP test could last between 1 h and 3 h. From the polarization curve, several parameters of importance can be extracted. The E20 and E200 represent values of breakdown potential and ER10, ER1 and ERCO represent values of repassivation potential.

RESULTS

Immersion Tests

Table 2 shows the corrosion rate results from the immersion testing. For all three types of coupons (ASW, LPB and LSP) the corrosion rate was the same. The highest average corrosion rate corresponded to the ASW coupons and the lowest to the LSP coupons but considering the standard deviation (SD), the corrosion rate values are indistinguishable from each other. Besides the data reported on Table 2, the corrosion rate of the base metal of the plates (away from the weld) in ASTM G 28 was also measured. The corrosion rate of the base metal was found to be 1.83 mm/year, which was higher than that of any of the welded coupons. It has been previously reported that the corrosion rate of as-welded 0.125-inch thick sheets of Alloy 22 in ASTM G 28A was 1.08 mm/year. [14] The standard corrosion rate of Alloy 22 given in a commercial brochure is 1.016 mm/year. 2 The common acceptance criterion for the maximum allowed corrosion rate for Alloy 22 is 80 mpy or 2 mm/year. 15

Table 2.
Immersion Corrosion Rates

Material	Coupon ID	Corrosion Rate, mm/year (mpy)	Average CR ± SD mm/year
ASW	W13-S1	1.26 (49.6)	1.303 ± 0.040
ASW	W14-S1	1.31 (51.48)	
ASW	W15-S1	1.34 (52.72)	
LPB	B9-S2	1.37 (54.02)	1.295 ± 0.106
LPB	B10-S2	1.22 (48.12)	
LSP	P13-S2	1.32 (52.07)	1.257 ± 0.055
LSP	P14-S2	1.23 (48.41)	
LSP	P15-S2	1.22 (47.86)	

After the corrosion immersion tests each specimen was thoroughly inspected under optical microscopy (stereomicroscope). All three type of materials suffered intergranular attack (IGA) in the heat affected zone (HAZ). The obvious IGA in the HAZ appears as black strips on each side of the weld seam (Figure 1). The IGA in the HAZ seemed less defined in the LSP coupons than in the ASW coupons.

Figures 2-3 show the aspect of the ASW corroded coupons, both in the base metal. Figure 2 represents the base metal away from the weld seam, which is the part of the plate that was not affected by the welding process. Figure 2 shows shallow and sporadic IGA. Figure 3 shows the aspect of corrosion in the HAZ, which is a couple of millimeters from the edge of the weld seam. Figure 3 shows more pronounced IGA probably promoted by second phase precipitation due to the exposure of the HAZ to intermediate temperatures (600 to 900°C) for the time involved in the welding process. [14-15]

Figure 4 shows the HAZ of a LPB corroded coupon. The aspect of Figure 4 is similar to that of Figure 3 showing that LPB treatment did not decrease the corrosion characteristics of an untreated welded plate (ASW). Figure 5 shows the HAZ of a LSP corroded coupon. It appears that the localized corrosion in the HAZ was different in the LSP coupon (Figure 5) than in the ASW and LPB coupons (Figures 3 and 4). At this moment it cannot be speculated what mechanism could have changed the mode of attack of the LSP coupons.

Figure 1. Corroded ASW Coupon W13-S1

Electrochemical Tests

The Corrosion Potential: Figure 6 shows the average E_{corr} for the three types of material after 24-hour immersion in deaerated 1 M NaCl at 90°C. E_{corr} was practically the same for all three materials ASW, LPB and LSP, that is, all the materials behaved similarly when immersed in hot saline solutions.

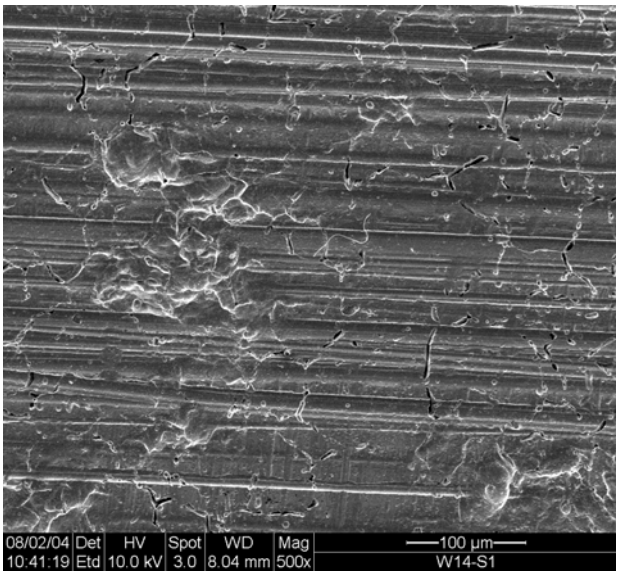

Figure 2. Corroded ASW Coupon W14-S1

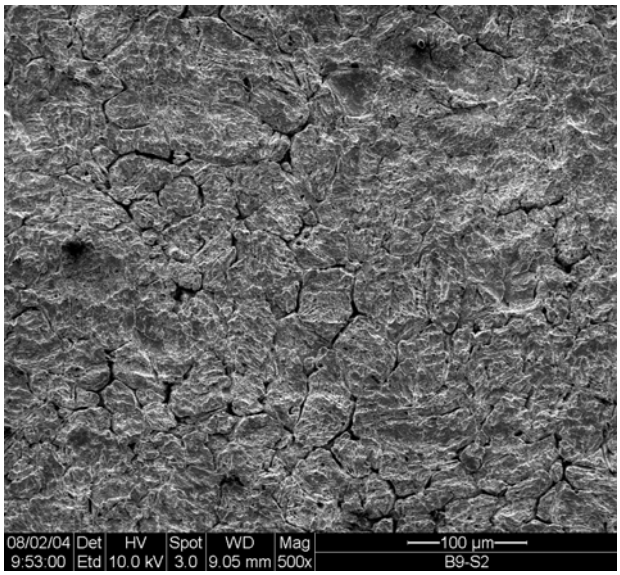

Figure 4. Corroded LPB Coupon B9-S2

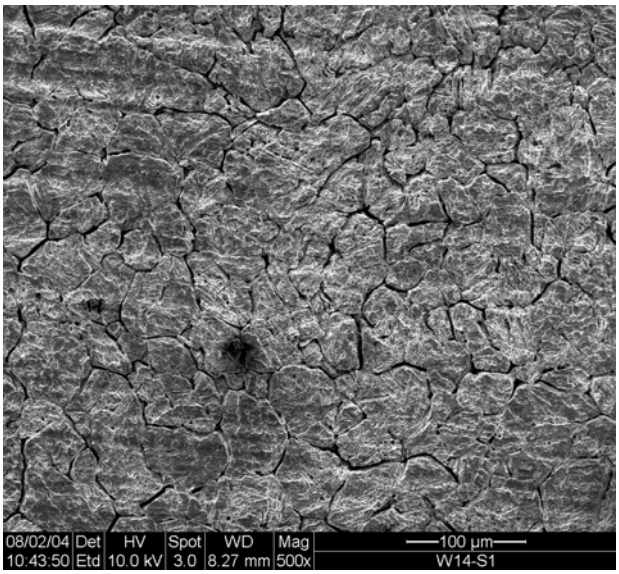

Figure 3. Corroded ASW Coupon W14-S1

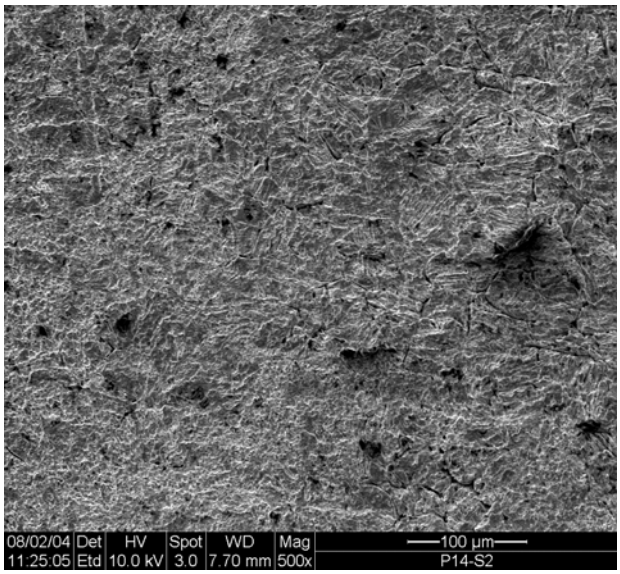

Figure 5. Corroded LSP Coupon P14-S2

The Corrosion Rate from Rp Measurements: The average corrosion rates in deaerated 1 M NaCl at 90°C were 0.208 ± 0.039, 0.188 ± 0.021 and 0.330 ± 0.121 µm/year for ASW, LPB and LSP, respectively. and in 6 m NaCl + 0.9 m KNO3 solutions, respectively. Considering standard deviations, the corrosion rate values for ASW, LPB and LSP calculated according to ASTM G 59 and G 102 cannot be differentiated from each other.

Cyclic Potentiodynamic Polarization (CPP): Figure 7 shows the cyclic potentiodynamic polarization curves for the three tested materials in deaerated 1 M NaCl pH 6 at 90°C. The behavior of all these materials was practically the same. Figures 6 shows E_{corr} and the parameters from the CPP curves for 1 M NaCl at 90°C. The breakdown potentials (E20 and E200) seemed slightly higher for LPB than for ASW and LSP materials. However, the repassivation potentials (ER1 and ERCO) seemed higher for the ASW material. The difference in potential values between the three materials is small enough to be considered

within experimental error. Figure 6 also shows that for the three tested conditions, the repassivation potential (ER1) was more positive than the corrosion potential (E_{corr}).

All the tested material suffered crevice corrosion when they were anodically polarized in 1 M NaCl at 90°C solution. The attack in the base metal is generally intergranular attack (IGA) or crystalline attack and in the weld seam it is interdendritic attack (IDA) (Figure 8). The type of attack did not change from the ASW to the LPB and LSP specimens. A more complete explanation of the findings is available elsewhere, [16]

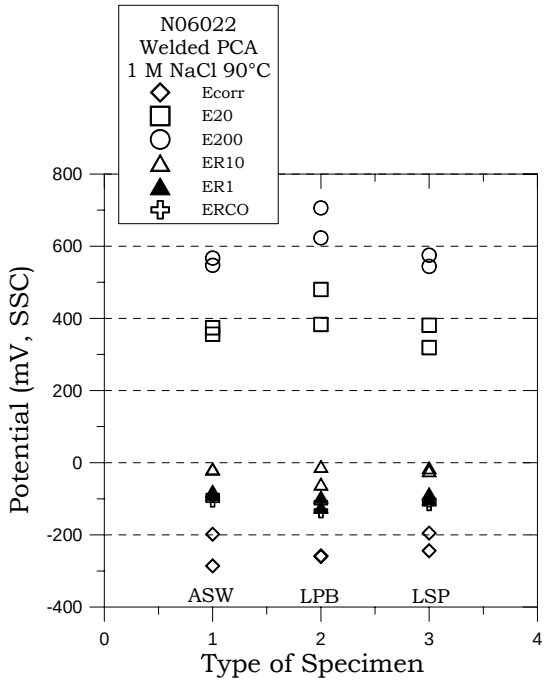

Figure 6. Parameters from CPP

CONCLUSIONS

- Surface tensile stress mitigation processes such as low plasticity burnishing (LPB) and laser shock peening (LSP) do not affect the corrosion resistance of welded Alloy 22 plates.

- Immersion tests in standard G 28 A solution showed that the corrosion rate by weight loss was the same for as-welded (ASW) material as for LPB and LSP materials

- Electrochemical tests such as cyclic potentiodynamic polarization showed that the anodic behavior of the three tested materials (ASW, LPB and LSP) was the same

The repassivation potential in chloride solutions of the three materials was the same

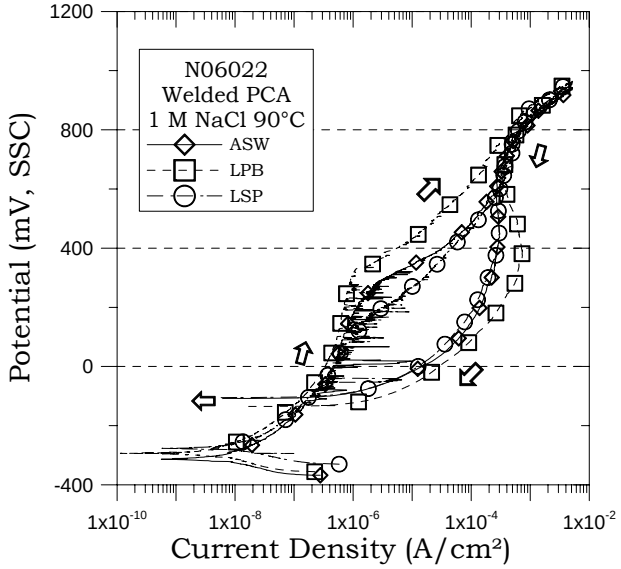

Figure 7. CPP of ASW, LPB and LSP Alloy 22

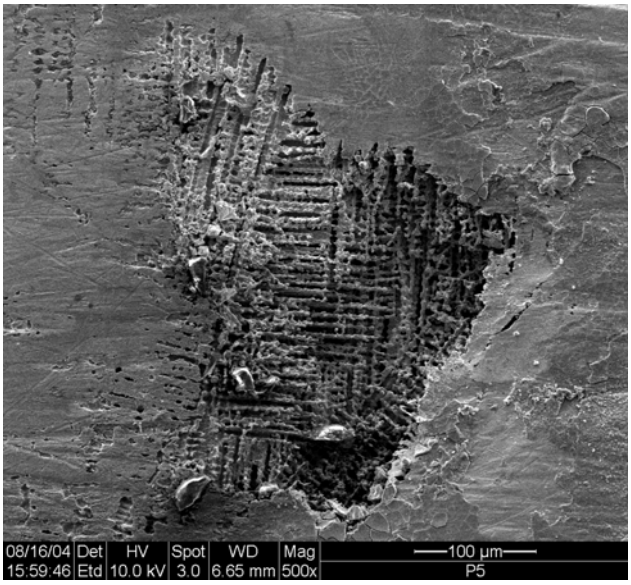

Figure 8. Interdendritic Attack (IDA) of Specimen P5 under the crevice former in 1 M NaCl at 90°C

ACKNOWLEDGMENTS

This work was partially performed under the auspices of the U. S. Department of Energy by the University of California Lawrence Livermore National Laboratory under contract W-7405-Eng-48. The work was supported by the Yucca Mountain Project, which is part of the DOE Office of Civilian Radioactive Waste Management (OCRWM).

DISCLAIMER

REFERENCES

1. ASTM International, Annual Book of ASTM Standards, Volume 02.04 “Non-Ferrous Metals” Standard 575 B (West Conshohocken, PA: ASTM International, 2002).
2. Haynes International, “Hastelloy C-22 Alloy”, Brochure H-2019E (Haynes International, 1997: Kokomo, IN)
3. R. B. Rebak, in Corrosion and Environmental Degradation, Volume II, p. 69, Wiley-VCH, Weinheim, Germany (2000)
4. R. B. Rebak and P. Crook, Advanced Materials and Processes, February 2000
5. Yucca Mountain Science and Engineering Report, U. S. Department of Energy, Office of Civilian Radioactive Waste Management, DOE/RW-0539, Las Vegas, NV, May 2001
6. G. M. Gordon, Corrosion, 58, 811 (2002)
7. S. C. Lu, G. M. Gordon and P. L. Andresen, PVP-Vol. 483, Transportation, Storage and Disposal of Radioactive Materials (American Society of Mechanical Engineers, 2004: New York, NY)
8. ASTM International, Annual Book of ASTM Standards, Volume 03.02 “Wear and Erosion; Metal Corrosion” p. 91 (West Conshohocken, PA: ASTM International, 2004)
9. U.S. Patents 5,826,453 (Oct. 1998), 6,415,486 B1 (Jul. 2002)
10. P. S. Prevéy, R. A. Ravindranath, M. Shepard and T. Gabb “Case Studies of Fatigue Life Improvement Using Low Plasticity Burnishing in Gas Turbine Engine Applications,” Proc. Of ASME Turbo Expo 2003, 16-19 June 2003, Atlanta, GA
11. C. S. Montross, T. Wei, L. Ye, G. Clark and Y.-W. Mai “Laser Shock Processing and its Effects on Microstructure and Properties of Metal Alloys: a Review,” International Journal of Fatigue, 24, 1021-1036 (2002)
12. M. R. Hill, A. T. DeWald, L. A. Hackel, H.-L. Chen, R. C. Specht and F. B. Harris “Laser Peening Technology,” Advanced Materials and Processes, 8, p. 65 (2003)
13. K. J. Evans, A. Yilmaz, S. D. Day, L. L. Wong, J. C. Estill and R. B. Rebak “Comparison of Electrochemical Methods to Determine Crevice Corrosion Repassivation Potential of Alloy 22 in Chloride Solutions,” JOM, p. 56, Jan. 2005.
14. R. B. Rebak, T. S. E. Summers, T. Lian, R. M. Carranza, J. R. Dillman, T. Corbin and P. Crook “Effect of Thermal Aging on the Corrosion Behavior of Wrought and Welded Alloy 22,” Corrosion/2002, Paper 02542 (NACE International, 2002: Houston, TX)
15. R. B. Rebak, T. S. E. Summers and R. M. Carranza, “Mechanical Properties, Microstructure and Corrosion Performance of C-22 Alloy Aged at 260°C to 800°C, Scientific Basis for Nuclear Waste Management XXIII, Vol. 608, p. 109 (Materials Research Society, 2000: Warrendale, PA).
16. D. V. Fix, A. Yilmaz, L. L. Wong, J. C. Estill and R. B. Rebak, Paper 05606, CORROSION/2005 (NACE International, 2005: Houston, TX).